Extreme Mechanics Letters 41 (2020) 101002

Contents lists available at ScienceDirect

Extreme Mechanics Letters

journal homepage: www.elsevier.com/locate/eml

Machine learning-based design and optimization of curved beams for multistable structures and metamaterials

Fan Liu, Xihang Jiang, Xintao Wang, Lifeng Wang *

Department of Mechanical Engineering, Stony Brook University, Stony Brook, NY 11794, USA

ARTICLE INFO

Article history:
Received 2 July 2020
Received in revised form 17 August 2020
Accepted 21 September 2020
Available online 28 September 2020

Keywords:
Structural optimization
Machine learning
Curved beam
Bistable
Metamaterials

ABSTRACT

Curved beams have been wildly used in MEMS (Micro-electromechanical systems) devices and energy absorption materials owing to its bistability. Almost all curved beams in previous studies have a constant thickness. Although better performance can be achieved by changing the thickness distribution, such as beams of uniform strength, lack of design and optimization tool limits the development and application of curved beams with varying thickness. In this paper, we demonstrate a new approach to design and optimize curved beams based on machine learning, which has been successful in many fields owing to its ability to process big data that can also be used in structural design and optimization. This machine learning-based model is able to achieve accurate predictions of nonlinear structure–property relationships. The optimized designs with different optimization objectives, such as stiffness, forward snapping force, and backward snapping force, are obtained efficiently and precisely. Experimental testing is conducted on specimens with optimized profiles, which are fabricated using a high-resolution multi-material 3D printer. The computational results are validated by the experimental results. The machine learning-based optimization approach developed here can provide a promising tool for the design and optimization of beam-based structures and mechanical metamaterials.

1. Introduction

A beam is a structural element that has been studied for many years and widely used in various engineering fields across length scale. In many large-scale structures, beams are used as horizontal structures to carry vertical loads, such as keels in ship structures and girders in bridge structures. Also, for microstructures, curved beams are used to construct architected metamaterials for energy trapping owing to its bistability [1–5]. From rectangular section beams to I beams, uniform cross-section beams to tapered beams, and straight beams to curved beams, engineers modify the form and shape of the beam to achieve different objectives. Newly developed fabrication techniques provide advanced tools to fabricate structure with complex geometries [6–8]. Meanwhile, rapidly developing industries bring up new demands to structures, such as to be lightweight and antifatigue. Therefore, how to use these tools to realize the various optimization objectives becomes essential.

For a given structure, its mechanical performance can be obtained using experimental testing or numerical simulations. However, the inverse problem, finding the structure to achieve a target performance is not straightforward as the design space is too large to be explored extensively. To solve the inverse problem, various optimization techniques have been developed, such as density method [9], level set method [10], and evolutionary approach [11]. These techniques achieve great success not only in mechanical design problems but also in other physical disciplines such as fluids and acoustics [12,13]. However, there are still many challenges including the high computational expense, the limited application range of compliance minimization problems, and the difficulty to apply more geometric and physical constraints [14].

The term "Machine Learning (ML)" was first coined by Arthur Samuel back in the 1950s when he created a checkers-playing program that can learn by itself [15]. With the rapid progress of computer hardware and the development of novel machine learning methods, ML has achieved great success in image recognition [16], speech recognition [17], medical prediction [18], and recommendation engines [19], and so on. The core ability of ML is that it can detect and reconstruct the complex internal correlations of input and output variables from a large-scale dataset. Therefore, in principle, the correlations between the shape of a structure and the performance of the structure can also be obtained by ML. Moreover, the corresponding optimization of the shape of the structure can be performed easily after establishing the correlations. This idea has already inspired researchers to apply ML to several optimization problems in different physical systems [20–26]. For example, the inverse design of graphene kirigami has been performed using NN and CNN machine learning

* Corresponding author.
E-mail address: lifeng.wang@stonybrook.edu (L. Wang).

https://doi.org/10.1016/j.eml.2020.101002
2352-4316/

models [20]. The optimal designs that maximize elastic stretchability have been obtained from a large design space with a small amount of training samples. Super-compressible metamaterials have been designed and optimized based on the Bayesian machine learning technique [22]. With the delicate design, brittle polymers have been transferred to lightweight and recoverable metamaterials. Hierarchical composites made of stiff and soft materials have been designed using convolutional neural networks [23]. The optimized patterns of the composites show significant increases in both strength and toughness. These studies demonstrate that ML can be a powerful tool in solving the inverse problem and designing structures with optimized performance. However, for the topic of beam optimization, the research is limited to optimizing parameters that are used to define limited shapes or profiles but not exhaustively searching the entire design space [27–30].

In this work, we focus on the design of the curved beam with a varied thickness distribution and the optimization of three mechanical objectives: stiffness (E), forward snapping force (S), and backward snapping force (B). We present an inversed design approach using fully connected neural networks and an optimized shape generator. We first describe the general mechanical performance of a curved beam and the concept of changing its performance by thickness modulation. Then we discuss the input training data creation for the machine learning model and the output training data distributions. Later, we propose the procedures of constructing an ML model and discuss the training process, verification process, and optimization process. After that, we show the training and optimization results of our ML model and show the optimized profiles of the beam for different optimization objectives. Finally, we fabricate specimens of beams with optimized profiles using a high-resolution multi-material 3D printer and perform validation tests on the specimens.

2. Mechanical properties of curved beams

Bistable mechanisms are widely used in designing microelectromechanical systems (MEMS) such as valves and switches since these devices need two stable positions to fulfill their functionalities. Also, bistable mechanisms are used to construct architected metamaterials for energy trapping. A typical bistable structure is a compressed straight beam which is very common in daily life, such as a compressed poker card with two stable positions. The bistability in a compressed straight beam is achieved by pre-applied stress, however, which is hard to fabricate. On the other hand, a curved beam with pre-shaped curvature may have bistability with carefully selected geometries. As shown in Fig. 1(a), the initial shape of the curved beam is:

$$w(x) = \frac{h}{2}\left[1 - \cos\left(2\pi\frac{x}{l}\right)\right] \tag{1}$$

where l is the span and h is the apex height of the beam. With the boundary condition as shown in Fig. 1(a) and with the second mode constrained, the typical load–displacement curve of this curved beam is shown as the blue line in Fig. 1(b). The highly nonlinear load–displacement curve has 3 stages: force increases in stage 1, decreases in stage 2, and increases again in stage 3, which can be explained by the change of bending and compression energy. Three mechanical properties of the curved beam can be extracted from the load–displacement curve: stiffness (E), which is determined by the initial slope of the load–displacement curve; forward snapping force (S), which is determined by the maximum force at the end of stage 1; backward snapping force (B), which is determined by the minimum force at the end of stage 2. The curved beam is bistable if the value of the backward snapping force is below 0. The effect of initial shape, such as curvature, on the mechanical properties of the curved beam has been investigated in previous studies. However, the mechanical properties can also be controlled and tuned by changing the thickness distribution of the beam. Here is an example: a curved beam with varying thickness as shown in Fig. 1(a). For the purpose of comparison between the mechanical properties of the beam with constant thickness and the beam with varying thickness, the initial shapes and the mass of the two beams remain the same. Fig. 1(b) shows two load–displacement curves, respectively. Clearly, by changing the thickness distribution, stiffness, forward snapping force, and backward snapping force can all be tuned. Now the question is: how to arrange the thickness distribution to achieve a desired mechanical performance?

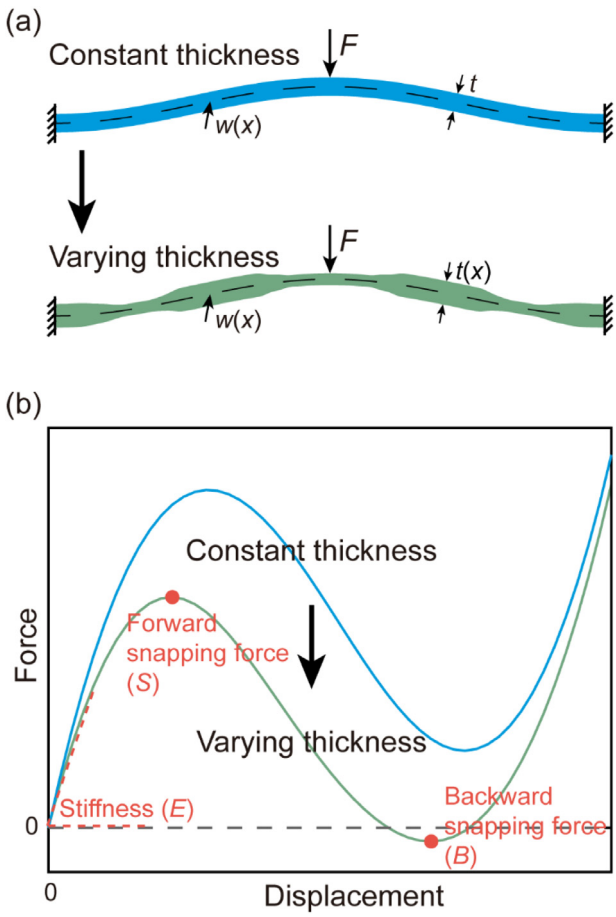

Fig. 1. Schematic diagrams of curved beams and typical load–displacement curves. (a) Geometry and notation for curved beams with constant thickness and varying thickness. (b) Typical load–displacement curves and three mechanical properties: stiffness (E), forward snapping force (S), and backward snapping force (B). . (For interpretation of the references to color in this figure legend, the reader is referred to the web version of this article.)

3. Machine learning model

In this section, an ML based model will be constructed, and the optimization based on the ML model will be performed. Fig. 2 shows a 4-step workflow used to construct the ML-based model. The first step is to create a database including two parts: beam profiles (input data) and mechanical properties (output data). The reference beam used for optimization has the following normalized geometric parameters: $l = 60$, $t = 2$, and $h = 8$. By changing the constant t to varying $t(x)$, there is an infinite number of beam profiles. To avoid unpractical designs that thickness is too thin in

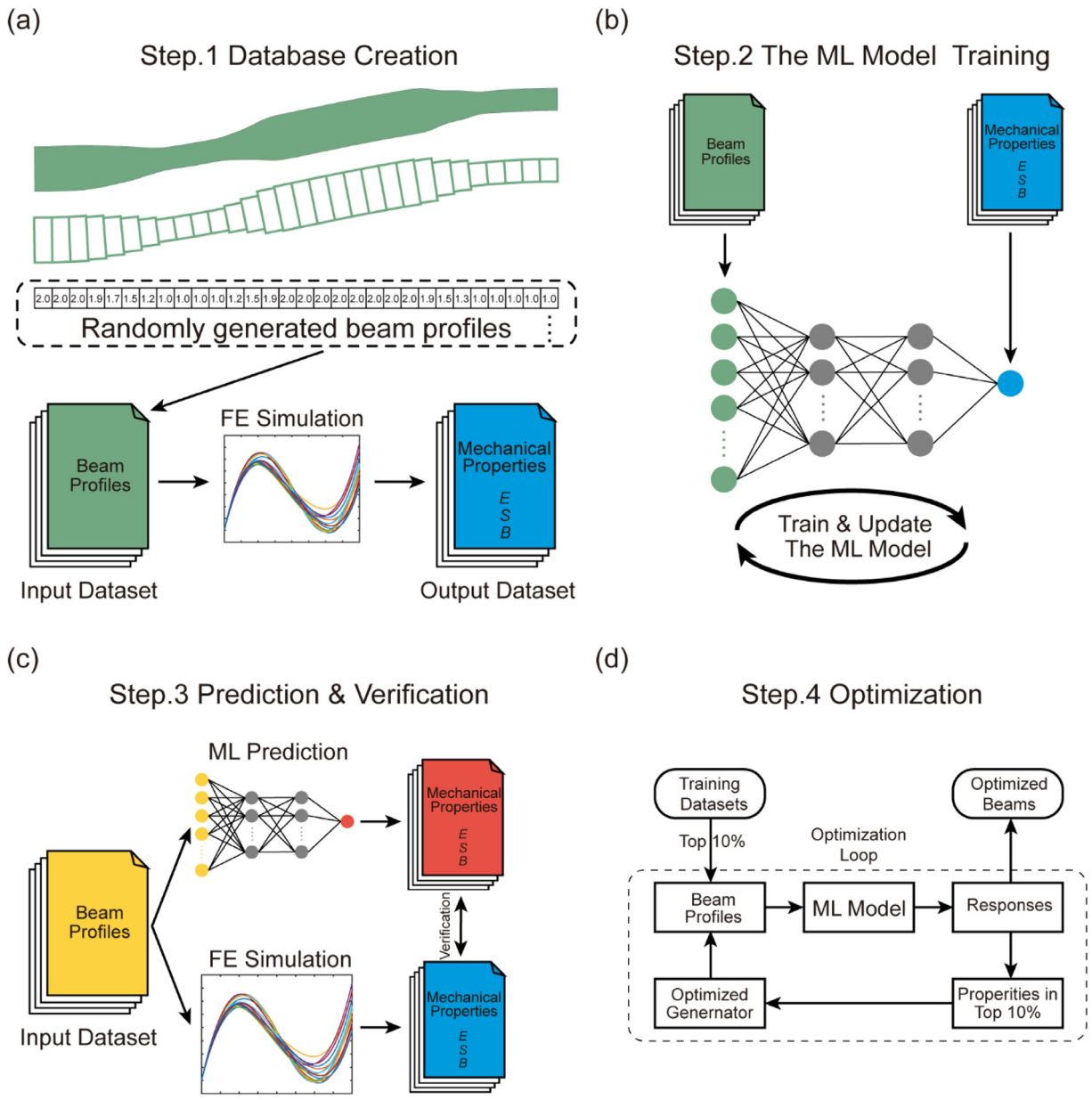

Fig. 2. The 4-step workflow of ML-based optimization of curved beam thickness distribution. (a) Training database creation. (b) The training process of the ML model. (c) The prediction and verification process of the ML model. (d) The flow chart of the optimization process.

some sections of the beam, we add a constrain $t_{\max}/t_{\min} \leq 2$, which means that for each beam in the design space, the thickest part of the beam cannot be 2 times thicker than the thinnest part of the beam. Note that this number can be changed based on the need. Because of the symmetric boundary condition, a half beam model is considered. The half beam model is then dispersed into 30 sections. An array with 30 numbers denotes the relative thickness of all 30 sections is used to describe the profile of the beam. The thinnest section has $t_i = 1$ while other sections has $t_i \in \{1.0, 1.1, 1.2, \cdots, 2.0\}$. The half beam model, discrete beam, and the relative thickness array are shown in Fig. 2(a). The input data used to train the ML model are relative thickness arrays. The output data, the mechanical properties of beams with different profiles, is obtained from finite element (FE) simulation results using Abaqus. The stiffness of the varying thickness beam can be obtained analytically [31]. However, it is hard to find analytical solutions to the highly non-linear mechanical properties of beams with complex profiles. Note that the relative thickness arrays must be transformed into real thickness arrays in the FE simulation. To ensure all beams have the same mass as the reference, the transformation is performed as:

$$t_i^o = \frac{t_i}{\sum_{i=1}^{30} t_i} \cdot 30 \cdot 2 \tag{2}$$

where t_i^o is the real thickness array and the t_i is the relative thickness array. Each possible beam profile has 30 sections and each section has 11 possible relative thicknesses. So, there are $\sim 11^{30}$ possible beam profiles in total, which is huge design space. Here, we randomly generate 10^5 beam profiles used as the input data and calculate 10^5 corresponding mechanical responses from FE simulation as output data. These are the data sets used to train the ML model.

After getting the database, the second step is to construct an ML model and use the database from the first step to train the model as shown in Fig. 2(b). An open-source neural-network library Keras [32] is used to construct the ML model. Firstly, the

type of the model should be determined. In this work, two types of models are considered: a sequential model and a convolutional neural networks model [32]. The ML model used in this work has one input layer with a size of 30×1, one output layer with the size of 1, and several hidden layers with different sizes. The number of hidden layers and the size of the hidden layers are tried with different numbers. Then, the loss function, which is a method of evaluating how well the algorithm models the database, needs to be determined. Moreover, two loss functions: mean squared error and mean absolute percentage error [32] are tried. Following this, a proper optimizer, which is used to shape and mold the model to a more accurate form during the training process, needs to be determined. Stochastic gradient descent optimizer and Adam optimizer [32] are used in this work. In the end, we try several activation functions for hidden layers and output layers including ReLU (Rectified Linear Unit) activation function, sigmoid activation function, and linear activation function [32]. At this point, a set of models can be constructed due to multiple combinations. In the training process, we test how well these models perform and determine one model that gives the most satisfactory result. Besides, we find the ideal values of weight matrices for all layers that minimize the loss function. Weight matrices are used to define the relationship between each layer in the ML model. Following these procedures, an ML model is constructed and trained which can well represent the relationship between the beam profiles and the mechanical properties in the training data sets.

The trained model in the previous step cannot be directly used for optimization because of the potential overfitting problem. As discussed previously, the whole design space is much larger than the training data sets. The ML model is intended to apply to the whole design space instead of just the training data sets. The ML model that fits the training data set well may not fit the whole design space. Therefore, another dataset that is independent of the training dataset is created with 10^4 random beam profiles. This dataset, which is known as the testing dataset, is used to verify the trained ML model. We use two methods to predict the mechanical properties of the 10^4 random beam profiles: FE simulation and the trained ML model, see Fig. 2(c). Two output datasets are therefore obtained. The loss function used in the training process is also used here to determine the difference between the two output datasets. The trained model can be validated if the value of loss calculated here is as small as the loss calculated in the training datasets.

In the last step, the trained and validated ML model is used to perform optimization. We follow the general optimization procedure proposed by [23]. The flow chart of optimization is shown in Fig. 2(d). In each optimization loop, 10^4 samples are predicted and evaluated by the ML model. Top 10% beam profiles in the training dataset are used as the initial samples in the first optimization loop. In the latter loops, 10^4 samples are generated based on evaluation results from the previous loop which includes three parts. The first part is 9000 beam profiles generated randomly. The second part is the top 100 samples from the previous loop. The third part is 900 samples generated based on the occurrence of relative thickness at each section in the top 10% samples from the previous loop. With several loops of optimization, beams with better mechanical performance can be obtained.

4. Results and discussion

As discussed in the first step, 10^5 beam profiles are randomly generated and the corresponding mechanical performances from FE simulation are calculated. Each simulation took $\sim$12 s on the Intel Xeon E5-1650 central processing unit (CPU). In this work. We have three optimization objectives: stiffness (E), forward snapping force (S), and backward snapping force (B). The histogram data of these three objectives are shown in Fig. 3 and all the results are normalized by the corresponding values of the reference beam (the beam with constant thickness). All three of them have roughly normal distributions. The goal of the optimization is to find beams exhibiting a higher value of stiffness, a higher value of forward snapping force, and a lower value of backward snapping force. As shown in Fig. 3(a–b), for stiffness and forward snapping force, the majority of beams in the training dataset show values lower than the beam with constant thickness. Considering the distribution of stiffness and forward snapping force, optimization objectives in the far-right tail region of the distributions are hard to obtain. Fig. 3(c) shows that distributions of the backward snapping force where beams with backward snapping force values lower than 0 are bistable beams which are marked with green. Though the beam with constant thickness is not a bistable beam, by changing the thickness distribution of the beam, bistability can be achieved.

With the training dataset, we have tried different ML models with the various parameters as discussed above. Grid-search is used to find the optimal parameters of a model that has the most accurate prediction. After performing a grid search on the number of the hidden layer (3 values), size of the hidden layer (10 values), and activation function (2 values), we obtain an optimal ML model that gives the most satisfactory result as shown in Fig. 4(a). It has one hidden layer with a size of 960. The activation functions used in the hidden layer and output layer are ReLU function and linear function, respectively. The loss function is mean squared error and the optimizer is Adam optimizer with a learning rate of 0.001. 100 epochs are used for training. The training process takes $\sim$40 m and each prediction based on the trained model takes $\sim10^{-4}$ s which is $\sim$100 000 times faster than FE simulation. The comparison between mechanical properties calculated by FE simulation and predicted by ML model is depicted in Fig. 4(b–d). Results from training datasets are shown with yellow dots that scatter around the straight-line $y = x$. It proves that the ML model has a high prediction accuracy for the training dataset. Also, results from testing datasets (blue dots) are scattered around the straight-line $y = x$ too, which demonstrates the ML model has no overfitting problem and can be used in the prediction and optimization for the entire design space. Note that a simple linear regression model can also be used to predict the structure-property relationships. However, it can not reach such high accuracy achieved by the ML model. The results of the top 100 high-performance designs after 10 loops and 100 loops of optimization are shown with pink and dark red dots. For the results after 10 loops optimization, all results are located in the high-performance range, but there are some overlaps with the training dataset. For the results after 100 loops optimization, the mechanical properties are further improved and there are no overlaps with the training dataset. That indicates the ML model we have trained with training datasets indeed has learned the designs with better performance. A beam design that has a stiffness 1.15 times higher and a forward snapping force 1.1 times higher than the reference beam can be obtained based on the parameters we use. The improvement of stiffness and forward snapping force is not very significant. However, the normalized backward snapping force value is changed from 1 to -1 after 100 optimization loops. Therefore, the bistability of a curved beam can be dramatically tuned by changing the thickness distribution.

Fig. 5 shows the results of beams with the optimized profiles and corresponding force–displacement curves using the ML-based optimization. The force is normalized by the forward snapping force of the reference beam and the displacement is normalized by 2 time the apex height of the beam $2h$. The first beam (red) has optimized forward snapping force and the second beam (green) beam has optimized stiffness. Both have similar

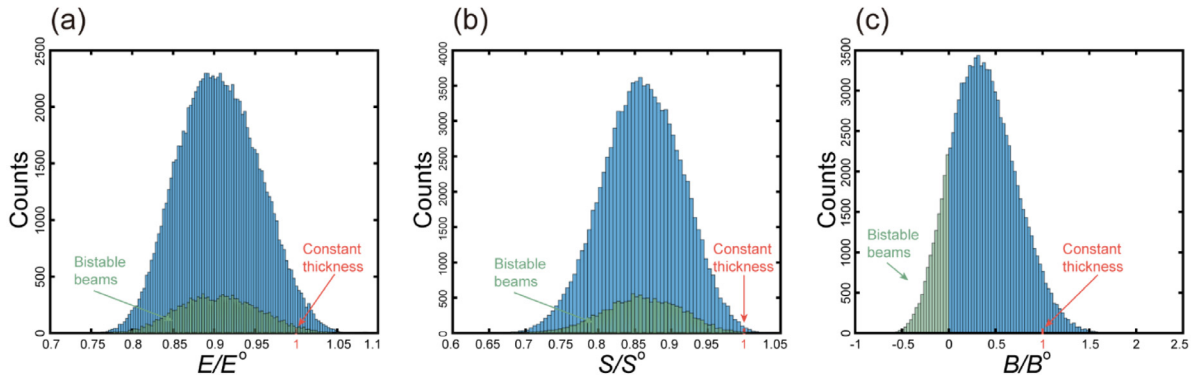

Fig. 3. Histogram of the three normalized optimization objectives in training dataset: (a) Stiffness (E). (b) Forward snapping force (S). (c) Backward snapping force (B). . (For interpretation of the references to color in this figure legend, the reader is referred to the web version of this article.)

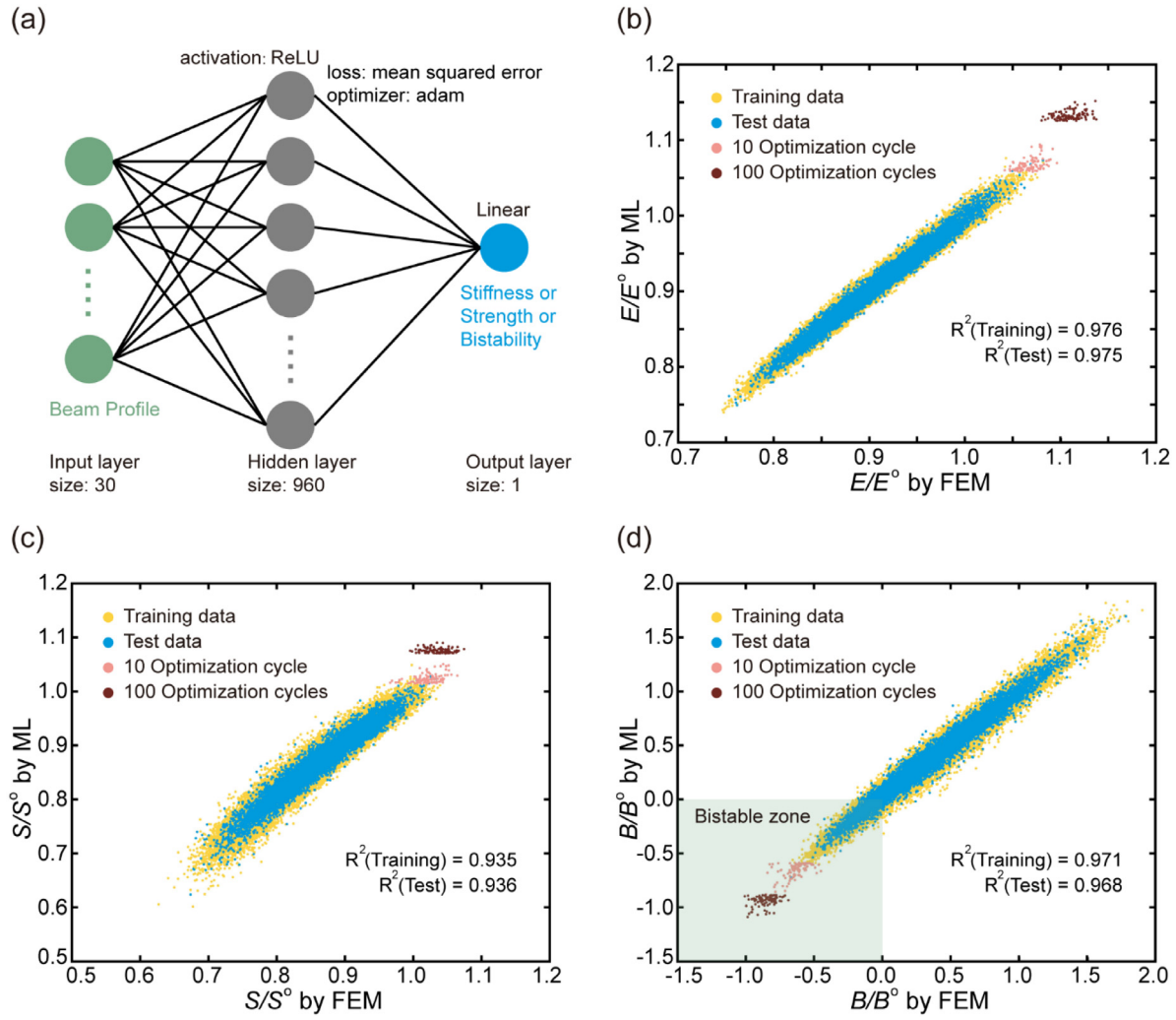

Fig. 4. Trained validated ML model and the optimization results. (a) Optimal ML model that gives the most satisfactory results. (b–d) Prediction and Optimization results based on the ML model for the three optimization objectives. . (For interpretation of the references to color in this figure legend, the reader is referred to the web version of this article.)

patterns of thickness distribution: thicker sections on both ends and thinner section in the middle. However, there is a slight difference between these two patterns. For the beam with optimized forward snapping force, the thickness changes gradually from thick to thin and the transition region is long. For the beam with optimized stiffness, thick sections change to thin sections dramatically in a very short region. Since stiffness is obtained at the small deformation of the test, high stress concentration can be found in both two ends of the beam. Optimized E design has thicker sections at both ends that could reduce the stress concentration and therefore increase the rigidity. However, under large deflection, the sudden thickness change in the optimized E design could create other stress concentration points, therefore generate a lower forward snapping force as compared to the

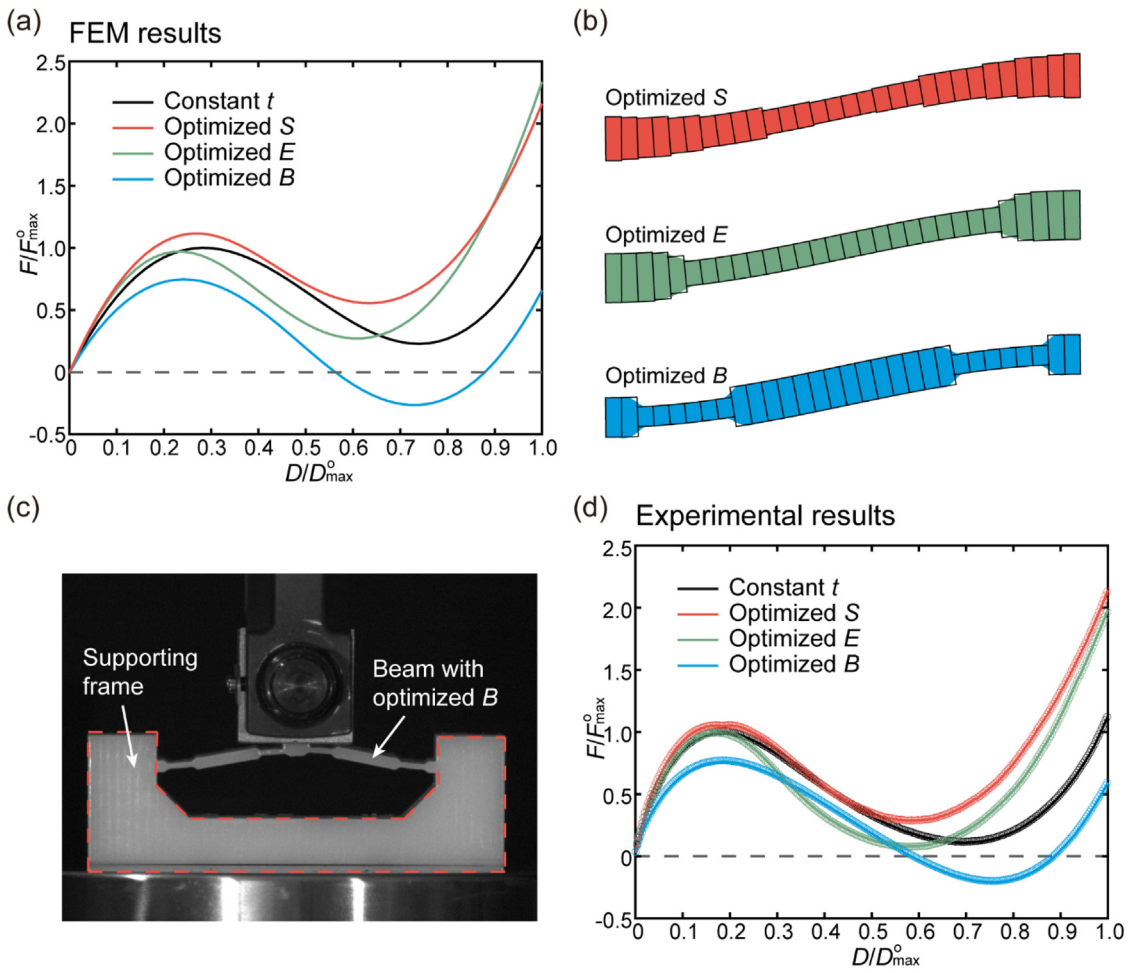

Fig. 5. Optimization results and experimental validation tests. (a) Optimized force–displacement curves for the reference beam with constant t and 3 optimized beams. (b) The corresponding beam profiles of 3 optimized beams. (c) A 3D printed beam specimen with optimized backward snapping force (B). (d) Experimental results of force–displacement curves for all 4 beams. . (For interpretation of the references to color in this figure legend, the reader is referred to the web version of this article.)

beams with optimized S. Note that both beams with optimized stiffness and optimized forward snapping force have positive backward snapping force values, indicating they are not bistable beams. The third beam (blue) is optimized to have the lowest backward snapping force value. Contrary to the previous two beams, the optimized bistable beam has thicker sections in the middle and thinner sections on both ends. The bistability mechanism of the beam can be explained by the structural energy change during the deformation. The energy stored in the beam comprises both bending energy and compression energy. The bending energy increases monotonically. The compression energy increases to maximum when the beam is almost straight then decreases. For the reference beam, the decrease of compression energy is slower than the increase of bending energy and the total energy keeps increasing. Thus, the reference beam is not bistable. However, for the beam with optimized backward snapping force, the two ends of the beam have higher stress concentration during the deformation. By decreasing the thickness of the two ends, the increase of bending energy is lowered. Therefore, the increase of bending energy is slower than the decrease of compression energy and the total energy is decreasing. That leads to a negative backward snapping force and bistability. Note that the designs in Fig. 5 are obtained by performing 100 loops of optimization. It is highly possible that we can find better design after performing more loops of optimization. The designs are not the true optimal designs but they are extremely close after a convergence of the results is researched in the 100 loops of optimization. The design space is too large to simulate all possible designs and find the best one. But the designs we find here can properly guide the design of the beam profiles.

To verify the optimization results, the specimens of the reference beam and all 3 optimized beams are fabricated using an Objet Connex260 multi-material 3D printer (Stratasys, Ltd) as shown in Fig. 5(c). A rigid plastic material VeroWhite is used to for the supporting frame and a rubber-like flexible material Shore 95A is used to print the beam. The compression tests are performed using an MTS mechanical tester (C43 frame) with a 1 kN load cell and the test rate is 8 mm/min. To facilitate comparison, load–displacement curves from compression tests are normalized in the same way as in Fig. 5(a). Clearly, the FE simulation curves in Fig. 5(a) show a good match with the experimental results in Fig. 5(d) and get validated. It is consistent that the optimized E design has the highest stiffness, the optimized S design has the highest forward snapping force, and the optimized B design has the lowest backward snapping force, which is negative.

5. Conclusion

In this paper, we have developed an approach to design curved beams using an ML-based optimization technique. The complete procedures of the ML-based optimization are discussed. We create a database including an input dataset describing the

beam profiles and output dataset describing mechanical properties. Several ML models are constructed and one of them which gives the most satisfactory result is selected. The ML model is trained and verified using the training and testing datasets. A self-learning optimization approach based on the ML model is performed to predict the profile of beams with optimized stiffness, forward snapping force, and backward snapping force, respectively. Beams specimens with optimized profiles are fabricated using a high-resolution multi-material 3D printer and tested. The optimization results are validated by the experimental results. The ML model in this study is able to capture the inherent highly nonlinear structure–property relationships of the whole design space with a limited amount of training dataset, which makes the ML model-based optimization much faster than conventional methods. Moreover, this optimization method is almost universal for different optimization objectives. Our study demonstrates the machine learning-based model can provide a promising tool for the design and optimization of structures and mechanical metamaterials. It should be noted that the optimization approach demonstrated in this paper is a single objective optimization process. However, combining with conventional methods, such as weighted sum method and ε-constraint method, we believe ML could be a promising tool for multi-objective optimization as well.

Declaration of competing interest

The authors declare that they have no known competing financial interests or personal relationships that could have appeared to influence the work reported in this paper.

References

[1] S. Liu, A.I. Azad, R. Burgueño, Architected materials for tailorable shear behavior with energy dissipation, Extreme Mech. Lett. 28 (2019) 1–7.
[2] A. Rafsanjani, D. Pasini, Bistable auxetic mechanical metamaterials inspired by ancient geometric motifs, Extreme Mech. Lett. 9 (2016) 291–296.
[3] S. Shan, S.H. Kang, J.R. Raney, P. Wang, L. Fang, F. Candido, J.A. Lewis, K. Bertoldi, Multistable architected materials for trapping elastic strain energy, Adv. Mater. 27 (29) (2015) 4296–4301.
[4] B. Haghpanah, L. Salari-Sharif, P. Pourrajab, J. Hopkins, L. Valdevit, Multistable shape-reconfigurable architected materials, Adv. Mater. 28 (36) (2016) 7915–7920.
[5] K. Che, C. Yuan, J. Wu, H. Jerry Qi, J. Meaud, Three-dimensional-printed multistable mechanical metamaterials with a deterministic deformation sequence, J. Appl. Mech. 84 (1) (2017) 011004.
[6] T.D. Ngo, A. Kashani, G. Imbalzano, K.T. Nguyen, D. Hui, Additive manufacturing (3D printing): A review of materials, methods, applications and challenges, Composites B 143 (2018) 172–196.
[7] M. Vaezi, H. Seitz, S. Yang, A review on 3D micro-additive manufacturing technologies, Int. J. Adv. Manuf. Technol. 67 (5–8) (2013) 1721–1754.
[8] H. Bikas, P. Stavropoulos, G. Chryssolouris, Additive manufacturing methods and modelling approaches: a critical review, Int. J. Adv. Manuf. Technol. 83 (1–4) (2016) 389–405.
[9] M.P. Bendsøe, Optimal shape design as a material distribution problem, Struct. Optim. 1 (4) (1989) 193–202.
[10] M.Y. Wang, X. Wang, D. Guo, A level set method for structural topology optimization, Comput. Methods Appl. Mech. Engrg. 192 (1–2) (2003) 227–246.
[11] Y.M. Xie, G.P. Steven, A simple evolutionary procedure for structural optimization, Comput. Struct. 49 (5) (1993) 885–896.
[12] G.H. Yoon, J.S. Jensen, O. Sigmund, Topology optimization of acoustic–structure interaction problems using a mixed finite element formulation, Internat. J. Numer. Methods Engrg. 70 (9) (2007) 1049–1075.
[13] S. Kreissl, K. Maute, Levelset based fluid topology optimization using the extended finite element method, Struct. Multidiscip. Optim. 46 (3) (2012) 311–326.
[14] O. Sigmund, K. Maute, Topology optimization approaches, Struct. Multidiscip. Optim. 48 (6) (2013) 1031–1055.
[15] A.L. Samuel, Some studies in machine learning using the game of checkers, IBM J. Res. Dev. 3 (3) (1959) 210–229.
[16] Q.V. Le, Building high-level features using large scale unsupervised learning, in: 2013 IEEE International Conference on Acoustics, Speech and Signal Processing, IEEE, 2013, pp. 8595–8598.
[17] L. Deng, J. Li, J.-T. Huang, K. Yao, D. Yu, F. Seide, M. Seltzer, G. Zweig, X. He, J. Williams, Recent advances in deep learning for speech research at Microsoft, in: 2013 IEEE International Conference on Acoustics, Speech and Signal Processing, IEEE, 2013, pp. 8604–8608.
[18] G. Litjens, T. Kooi, B.E. Bejnordi, A.A.A. Setio, F. Ciompi, M. Ghafoorian, J.A. Van Der Laak, B. Van Ginneken, C.I. Sánchez, A survey on deep learning in medical image analysis, Med. Image Anal. 42 (2017) 60–88.
[19] A.M. Elkahky, Y. Song, X. He, A multi-view deep learning approach for cross domain user modeling in recommendation systems, in: Proceedings of the 24th International Conference on World Wide Web, 2015, pp. 278–288.
[20] P.Z. Hanakata, E.D. Cubuk, D.K. Campbell, H.S. Park, Accelerated search and design of stretchable graphene kirigami using machine learning, Phys. Rev. Lett. 121 (25) (2018) 255304.
[21] J.K. Wilt, C.X. Yang, G.X. Gu, Accelerating Auxetic Metamaterial Design with deep learning, Adv. Energy Mater. 22 (2020) 1901266.
[22] M.A. Bessa, P. Glowacki, M. Houlder, Bayesian machine learning in Metamaterial Design: Fragile Becomes Supercompressible, Adv. Mater. 31 (48) (2019) 1904845.
[23] G.X. Gu, C.-T. Chen, D.J. Richmond, M.J. Buehler, Bioinspired hierarchical composite design using machine learning: simulation, additive manufacturing, and experiment, Mater. Horiz. 5 (5) (2018) 939–945.
[24] G.X. Gu, C.-T. Chen, M.J. Buehler, De novo composite design based on machine learning algorithm, Extreme Mech. Lett. 18 (2018) 19–28.
[25] Z. Liu, C. Wu, Exploring the 3d architectures of deep material network in data-driven multiscale mechanics, J. Mech. Phys. Solids 127 (2019) 20–46.
[26] C.T. Chen, G.X. Gu, Generative deep neural networks for Inverse Materials design using Backpropagation and active learning, Adv. Sci. 7 (5) (2020) 1902607.
[27] J.M. Dietl, E. Garcia, Beam shape optimization for power harvesting, J. Intell. Mater. Syst. Struct. 21 (6) (2010) 633–646.
[28] M. Ohsaki, H. Tagawa, P. Pan, Shape optimization of reduced beam section under cyclic loads, J. Construct. Steel Res. 65 (7) (2009) 1511–1519.
[29] Y. Enns, E. Pyatishev, A. Glukhovskoy, Bistable arch-like beams with modulated profile as perspective supporting structures of a micro-electromenchanical actuator, IOP Conf. Ser.: J. Phys.: Conf. Ser. 917 (2017).
[30] I.-T. Chi, T.H. Ngo, P.-L. Chang, N.D.K. Tran, D.-A. Wang, Design of a bistable mechanism with B-spline profiled beam for versatile switching forces, Sensors Actuators A 294 (2019) 173–184.
[31] Y. Xu, D. Zhou, Elasticity solution of multi-span beams with variable thickness under static loads, Appl. Math. Model. 33 (7) (2009) 2951–2966.
[32] Keras, Keras API reference, 2020, https://keras.io/api/datasets/.